nature portfolio

Peer Review File

Chiral oxazolidinones via biocatalytic aziridination of unactivated alkenes

Corresponding Author: Professor Frances Arnold

Any redactions in this file are there to maintain patient confidentiality, the confidentiality of unpublished data, or to remove third-party material.

This file contains all reviewer reports in order by version, followed by all author rebuttals in order by version.

Version 0:

Reviewer comments:

Referee #1

(Remarks to the Author)
Arnold and co-workers submitted a manuscript describing the development of a biocatalytic method for constructing chiral oxazolidinones using engineered heme enzymes that catalyze an aziridination/ring-expansion cascade through nitrene transfer. The authors combined reaction discovery in a hemoprotein library with directed evolution to improve initial low yields and enantioselectivity. They also investigated a broad scope of substrates for nitrene transfer-enabled formation of diverse 5-(S)-aminomethyl oxazolidinones. Further directed evolution expanded the accessible product scope to include clinically relevant 5-(S)-aminomethyl oxazolidinones. Additionally, the authors performed mechanistic and computational studies to elucidate the reaction mechanism. Their results suggest that the hemoprotein-catalyzed reaction proceeds via a nitrene transfer mechanism, forming an enantioenriched aziridine intermediate followed by a stereoinvertive intramolecular SN2 reaction.

As the authors pointed out in the introduction to their article, chiral oxazolidinones emerged as promising treatments of multi-resistant pathogens. However, the antibacterial activity strikingly depends on the absolute 5-(S) configuration at the α-to-oxygen stereogenic center. Current synthetic methods toward this chiral synthon are costly and process-intensive. Methods for biocatalytically constructing the 5-(S) stereogenic center de novo are limited.
Therefore, the new method presented in this manuscript is of interest, as it uses readily available precursors and relies on only one catalytic step.

The research was carried out competently, and the presented data support the authors' conclusions, with only a few minor exceptions. The manuscript is well-structured and well-written. The experimental procedures are described in sufficient detail to allow others in the field to reproduce them, with a few exceptions. The reported reactions are conceptually noval and interesting. However, to showcase the synthetic utility of this transformation, the authors could have attempted to optimize the reaction conditions further, given that the obtained yields remain below 50% in most cases. Along those lines, one of the reactions toward a clinically relevant product (e.g., 3x or 3z) should have been demonstrated on a preparative scale to demonstrate synthetic utility. Additionally, it would have been important to characterize the best protein engineering variants (ApPgb-OxazS-G8-5409 and ApPgb-OxazS-G8) kinetically and report total turnover numbers (TTNs) to evaluate the operational stability of a biocatalyst.

Overall, this submission describes an innovative biocatalytic method for constructing chiral oxazolidinones. However, the manuscript does not yet reach the quality required for publication in Nature, taking into account the missing preparative-scale reactions, lack of further optimization to improve the yields, and missing kinetic data of improved biocatalysts to better judge synthetic utility at this stage.
Further suggestions for improving the manuscript are provided below.

Results & Discussion:
1. Page 4, lines98-103: For the initial screening, an in-house library of engineered hemoproteins was screened. First, it would be helpful to provide more information about the variants included in the initial screening. The authors describe how the initial activity of ApPgb-Oxazolidinone Synthase (OxazS)-G0-5401 was attributed to the F73W104 mutation in the B/E

tunnel. Meanwhile, ancestral variants lacking this mutation exhibited significantly diminished activity. However, since no information about the variants included in the screening is provided, it is impossible to compare the (OxazS)-G0-5401 enzyme with the other variants in the library. Additionally, more information and potentially a visualization of the B/E tunnel should be provided, as it may not be immediately clear to readers who are not experts in this particular hemoprotein class. Lastly, the authors refer to Table S8, which provides an overview of the initial screening with engineered protoglobin variants in a 96-well plate format. However, the reference to Table S8 is placed after the sentence about the B/E tunnel, which seems inappropriate since Table S8 does not offer additional information about the F73W mutation or the B/E tunnel.
2. Page 4, lines110-130: The authors describe their combined strategy of site-saturation mutagenesis, random mutagenesis, and a staggered extension process for recombination. This strategy allows them to navigate the sequence-function space, thereby increasing the yield and enantioselectivity of the chosen model reaction. While the overall engineering strategy is clear, it would be helpful to explain which residues were selected for saturation in the SSM approach, as well as how many were selected and why.
3. Figure 2b: The model shows the mutated residues of ApPgb-OxazS-G8-5409 compared to the residues of the ancestor, ApPgb-OxazS-G0-5401. To improve overall understanding and reproducibility, it would be helpful to add a table to the Supplementary Information with an overview of the wild-type mutations (specific residues), as well as the mutations introduced in variant G8.
4. Page 6, line194: The addition of a small amount of 1x to the benchmark reaction between 1a and 2a is mentioned here. This reduced the initial rate and showed evident substrate inhibition. However, the authors refer to Figure S3, which shows the results obtained with other nitrene precursors. This seems incorrect (must be Figure S4).
Supplementary Information:
1. Figure S2: Include information on the ee with which the target oxazolidinone was obtained
2. Page 18 and following: The authors should also include the calculated concentration [mM] of the respective products (can be added to the tables underneath the calibration curves).
3. Page 54: 5-(aminomethyl)-3-(p-tolyl)oxazolidin-2-one (3b): Please indicate if this compound was obtained from a commercial source or synthesized.
4. Page 61: tert-butyl (3-amino-2-hydroxypropyl)(p-tolyl)carbamate (5): The authors describe that this compound was synthesized according to the General Procedure C. However, I couldn't find a description of Procedure C in the SI. Please check and add a detailed description.

Referee #2

(Remarks to the Author)
This submission details a biocatalytic aziridination of a specific class of alkene – an N-Boc, N-aryl allyl amine. After aziridination with an aminating agent that initially leads to an unprotected aziridine, an internal rearrangement commences which opens the aziridine to form an oxazolidinone. This places the new stereocenter at the position alpha to oxygen in the oxazolidinone. The authors make the point that most methods to access oxazolidinones install stereocenters at the other position (alpha to N). Although they point out also that there exist established routes to this present class – most notably from the chiral pool building block epichlorohydrin, which is available extremely cheaply as single enantiomers.

For the optimization substrate 1a, exhaustive rounds of directed evolution are able to get the yield and ee to excellent levels (Fig 2). They then explore variation of the phenyl ring of the optimization substate to different substituted phenyls. The outcomes are quite a mix. Although good outcomes can be retained for some simple substitutions (eg p-CO2Me, m-OMe) for many the yields and the ee values decrease quite substantially and overall the scope, even of arene substitution, seems limited. Even though there are a good proportion from Fig 3 which give high ee, often the yields are low to moderate. The addition of a methyl group on the alkene gives only 2% yield and 40% ee, indicating that it has to be a terminal, monosubstituted alkene. The authors comment that this makes it a good starting point for a future campaign but it seems clear that the present system cannot deal with this effectively. In Fig 4 further rounds of evolution are carried out to permit a sulfur atom to be present. The remainder of the manuscript is largely computational and a computational reviewer would be needed to comment authoritatively on this aspect.
The title "Biocatalytic Nitrene Transfer Enables Aziridination of Unactivated Alkenes for the Synthesis of Chiral Oxazolidinones" sounds quite broad but the space within which the reaction operates is narrow (see above comments). Furthermore in the past couple of years there have been several asymmetric aziridination processes which operate very effectively on unactivated terminal alkenes with broad scope. For example, ref 36 in the submission, but also a paper which is not cited here (unless I missed it) from Baik and Blakey (JACS, 2024, 146, 1447) using Rh catalysis. Therefore, it is difficult to say this is unaddressed problem in the literature.

The rather restricted substrates that this delivers good results on (ie an N-Boc, N-aryl allyl amine, with relatively limited possibility to move away from Phenyl as the aryl group) means that it is not of the broad interest and impact level needed to justify publication in Nature, in this reviewers opinion. It is a nice study that is well executed. It is clear that a huge amount of work went into the directed evolution studies. But my opinion is that publication in JACS or ACS Central Science would more appropriate for the reasons stated above.

Referee #3

(Remarks to the Author)
The manuscript titled "Biocatalytic Nitrene Transfer Enables Aziridination of Unactivated Alkenes for the Synthesis of Chiral Oxazolidinones" by Frances H. Arnold and coworkers reports the development of a novel biocatalyst, OxazS G8, for the

enantioselective production of chiral oxazolidinones from inert alkenes via directed evolution of a heme-containing protein. Using both experimental optimization and computational analyses (DFT and MD), the authors demonstrate that this new enzyme efficiently catalyzes nitrene transfer and aziridination, opening promising possibilities for the direct and sustainable synthesis of clinically important antibiotics. The work is of high interest and, in my opinion, suitable for publication in Nature, but the clarity and impact of the manuscript would benefit from addressing the following minor points.
1. The authors observe a dramatic increase in reaction yield upon optimization of the experimental conditions for OxazS-G8. This improvement would be more informative if the same optimization protocol were also applied to the earlier OxazS-G8 variant that already achieved high enantioselectivity but much lower yield (Figure 2), to clarify whether the yield boost is primarily due to the new mutations or mainly to condition screening.
2. The computational studies focus on OxazS-G2 and OxazS-G3, but the rationale for selecting these specific variants is currently unclear. A brief explanation of why these were chosen for detailed analysis, rather than other members of the directed evolution trajectory, would help the reader follow the computational strategy.
3. The A59V mutation is close to the active site and appears important, but the roles of more distal mutations remain less clear. A more detailed discussion of whether these distal changes could exert allosteric effects, and how that might influence reactivity or selectivity, would add value to the mechanistic interpretation.
4. A table summarizing the atomic spin populations obtained from DFT calculations would be helpful for tracking the distribution of unpaired electrons throughout the reaction pathway and clarifying the electronic structure changes along the nitrene transfer and aziridination steps.
5. It would be informative to know whether kinetic rate constants can be extracted from the experimental data. If so, quantifying the catalytic improvement of the evolved variants relative to earlier ones would greatly strengthen the mechanistic narrative. If computed rates are available, it would also be useful to know which step is predicted to be rate-determining in the current variant.
6. The manuscript highlights a CH-π interaction that is said to be important for the reaction. Because such interactions are typically weak and have some electronic character, it would be helpful to clarify how their strength was assessed in the MD simulations and how confident the authors are that the chosen force field captures this effect adequately.
7. The MD protocol used to compare OxazS-G8 and StzS-G4 is notably different from the one applied elsewhere. A more consistent treatment across variants would aid direct comparison. In addition, showing computed tunnels on protein structures would help illustrate how the active site environment differs between these systems.
8. The role of the enzyme in the ring-expansion step is not fully explained. A more detailed description of how the protein environment facilitates (or avoids inhibiting) this step would improve understanding of the downstream transformation.
9. The blue surfaces shown in Figure S10 are not clearly described in the caption or main text. A brief explanation of what these surfaces represent (e.g., cavities or some other property) would be useful.
10. The confidence scores of the AF3-predicted structures should be provided.
11. The time evolution plots in Figures S11 and S13 show 0-1500 ns on the x-axis, but the trajectories appear to cover only 500 ns per replica. For clarity, I suggest rescaling the x-axis to 0-500 ns for each replica. In addition, the red line in these panels appears to represent a running average across replicas, which is misleading. It would be preferable either to show individual replicas distinctly or to clarify that the red line is an across-replica average.
12. The phrase “classical MD” is somewhat redundant, as MD simulations in this context are inherently classical, force field-based methods. Unless the study involved hybrid or quantum mechanical MD approaches, it would be more appropriate to simply refer to “MD” or reserve “classical MD” only when explicitly contrasting with quantum or ab initio MD.
13. The AMBER topologies, coordinates, and simulation input files should be deposited in an open access repository or provided as part of the supplementary data to ensure full reproducibility of the computational results.

Version 1:

Reviewer comments:

Referee #1

(Remarks to the Author)
I thank the authors for their careful and comprehensive responses to my comments and for the corresponding revisions to the manuscript and the supporting information. Overall, I am satisfied with the authors’ responses, and I believe that the manuscript has been substantially improved by the revisions. In particular, the authors have adequately addressed the major concerns raised in my previous report.

I only have a few remaining minor comments that I would ask the authors to address before publication. These points are detailed below and are primarily intended to further improve the clarity and accuracy of the manuscript.

Minor comments:
- Condition Optimization (Figure S15): What is shown on the y-axis? Please provide an axis description.
- Figure 2 in the main manuscript: It is unclear why the authors removed the amino acid substitution labels in Figure 2b. I believe these are important and should be added again.
- The authors have performed prep-scale synthesis of 3a, 3v, 3y, and 3z, which I very much appreciate. They added the following statement to the main manuscript: "Preparative-scale synthesis of selected examples was performed to demonstrate the utility of this methodology (see Supplementary Information, Table S16)." For clarity and an easier overview for the reader, I recommend specifically mentioning the selected examples 3a, 3v, 3y, and 3z in this sentence.

Subject to satisfactory consideration of these remaining minor points, I have no further concerns regarding the manuscript.

Referee #3

(Remarks to the Author)
I have no further questions. The authors have provided clear and thorough responses to all of my questions and have addressed the points raised in my initial review. In my opinion, the manuscript now meets the scientific and editorial standards of Nature, and I recommend it for publication.

Referee #1

We thank this reviewer for their supportive comments and valuable suggestions.

1. The reviewer writes: "To showcase the synthetic utility of this transformation, the authors could have attempted to optimize the reaction conditions further."
Response: The standard reaction condition was optimized for **3a**, during which we determined the major limitation was an issue with substrate solubility. With this in mind, we conducted substrate-specific condition optimization using **3v** as a benchmark. Factors including variety and volume % of co-solvent, reaction temperature, and surfactant were taken into consideration. Slightly increasing the v% of ethanol to 10% gives slightly increases product yield. Adding surfactant or increasing the reaction temperature also gives slightly improved activity. Other solvents such as DMF and *i*-PrOH were also compatible, while acetone and acetonitrile are deleterious. This data has been added to the supporting information (Table S15). We are optimistic that the reaction can be improved further with more effort and expertise. However, we hope you agree that process development is out of the scope of this initial, methodology-oriented study.

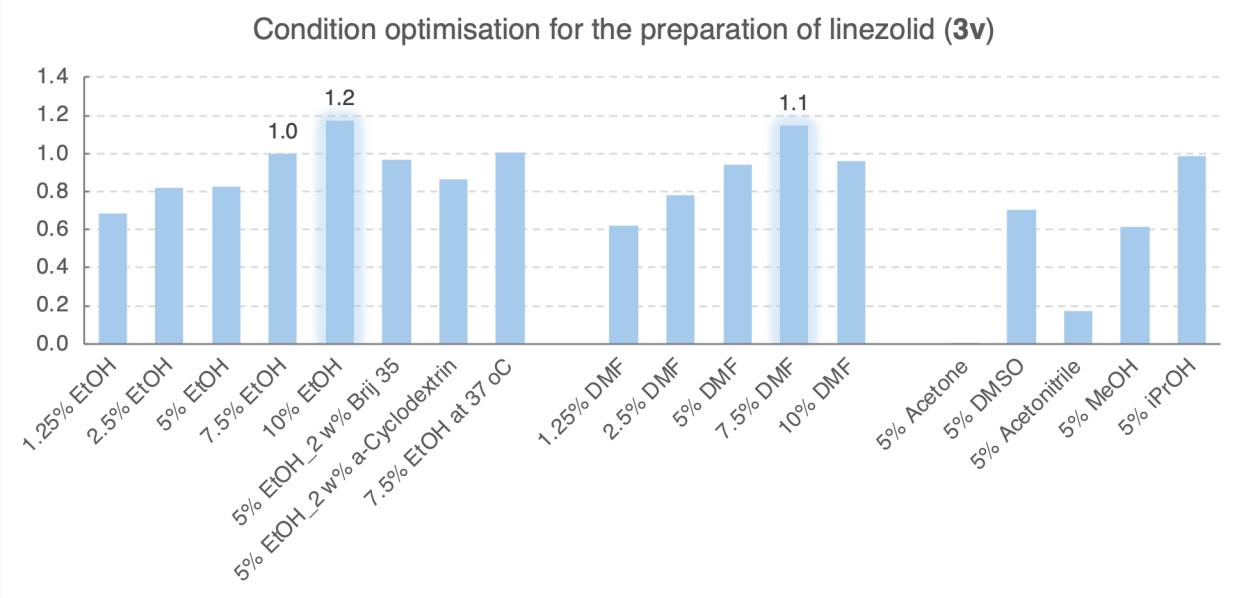

Figure S15. Condition optimization using linezolid (**3v)** as an example.

2. The reviewer writes: "One of the reactions toward a clinically relevant product (e.g., 3x or 3z) should have been demonstrated on a preparative scale to demonstrate synthetic utility."

Response: To demonstrate the synthetic utility of the transformation, we have performed preparative scale synthesis of **3a**, **3v**, **3y**, and **3z**. We added a section in the supporting information to describe the protocol for the preparative reaction set-up and product quantification.

Table S16. Preparative-scale synthesis of selected oxazolidinones.

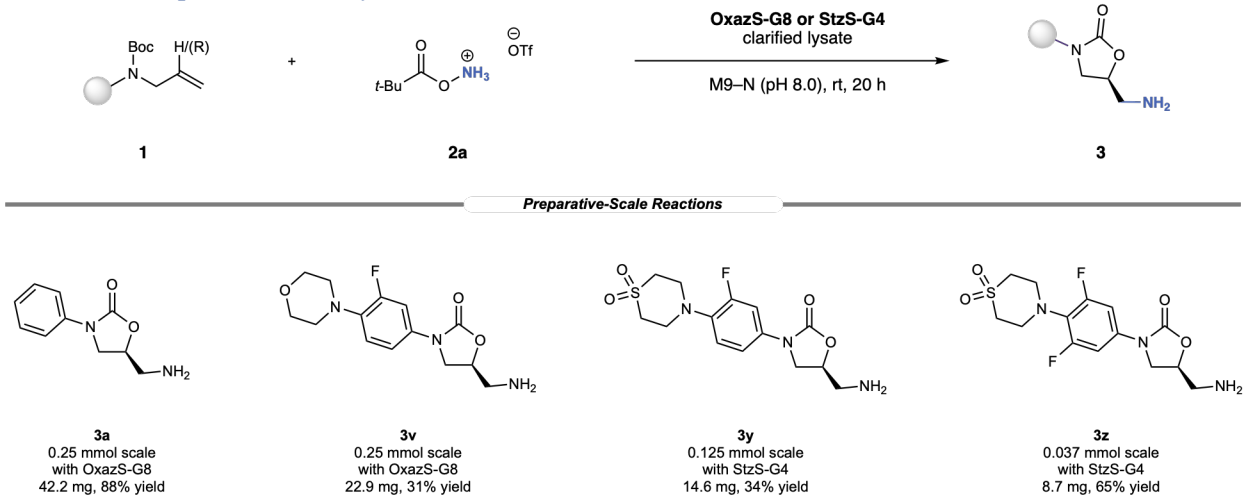

3. The reviewer writes: "it would have been important to characterize the best protein engineering variants (ApPgb-OxazS-G8-5409 and ApPgb-OxazS-G8) kinetically and report total turnover numbers (TTNs) to evaluate the operational stability of a biocatalyst."

Response: We thank the reviewer for this suggestion. The product is generated through a two-step cascade involving an aziridine intermediate that cannot be directly detected or quantified. Consequently, the rate of final-product formation reflects the combined kinetics of intermediate formation and subsequent conversion

rather than an individual enzyme-catalysed step. Moreover, because the transformation proceeds over an extended period and is influenced by substrate solubility and aminating-reagent decomposition, conventional steady-state Michaelis–Menten parameters may not provide a straightforward (or even useful) description of catalytic performance under different reaction conditions. To avoid overinterpretation, we instead report time-course data in Fig. S5 as measures of the overall catalytic performance under the reaction conditions.

To measure TTNs, we used the hemochrome assay to determine heme (and thus active catalyst) concentration (General information, section D). The representative heme concentration for ***Ap*Pgb-OxazS-G8-5409** was 10.5 μM and for ***Ap*Pgb-StzS-G4-5413** was 5.3 μM. We controlled OD_{600} = 50 before sonication for preparation of clarified cell lysate. Heme concentrations can vary slightly from batch to batch. We added TTNs for selected examples to the supporting information. For example, **3a** was produced in 197 TTN when the reaction was performed at 5 mM substrate concentration.

4. The reviewer writes: 1) "Page 4, lines 98-103: For the initial screening, an in-house library of engineered hemoproteins was screened. First, it would be helpful to provide more information about the variants included in the initial screening." 2) "The initial activity of *Ap*Pgb-Oxazolidinone Synthase (OxazS)-G0-5401 was attributed to the F73W mutation in the B/E tunnel. …However, since no information about the variants included in the screening is provided, it is impossible to compare the (OxazS)-G0-5401 enzyme with the other variants in the library." 3) "More information and potentially a visualization of the B/E tunnel should be provided, as it may not be immediately clear to readers who are not experts in this particular hemoprotein class." 4) "Lastly, the authors refer to Table S8, which provides an overview of the initial screening with engineered protoglobin variants in a 96-well plate format. However, the reference to Table S8 is placed after the sentence about the B/E tunnel, which seems inappropriate since Table S8 does not offer additional information about the F73W mutation or the B/E tunnel."

Response: 1) The initial screening was conducted using an in-house library containing but not limited to wild-type protoglobin homologues and evolved hydroxylamine nitrene transferases reported in *J. Am. Chem. Soc*. **2023**, *145*, 20196–20201; α-amino ester synthases reported in *J. Am. Chem. Soc.* **2024**, *146*, 27267–27273; boronic acid aminase reported in *J. Am. Chem. Soc.* **2024,** *146*, 19160–19167; cyclopropanase reported in *J. Am. Chem. Soc.* **2025**, *147*, 27165–27171; and other unpublished variants. This paragraph was added to the supporting information, initial reaction discovery section.

2) The highest initial activity was observed using previously reported variant L-*Ap*Pgb-αEsA-G9 (D11 in a 96-well compilation plate, later designated *Ap*Pgb-OxazS-G0). A critical mutation F73W was introduced compared to its ancestral variants (Ref: *J. Am. Chem. Soc.* **2024**, *146*, 27267–27273). This information has been added to the supporting information **Table S9**.

Well No.	Mutations compared to ***Ap*Pgb-wt**
D1	W59A_Y60G_F145G_F156L
D2	W59A_Y60G_I97T_F145G_F156L
D3	W59A_Y60G_I97T_F145G_F156L_F175L
D4	W59A_Y60G_I97T_I137T_F145G_F156L_F175L
D5	W59A_Y60G_I97V_I137T_F145G_F156L_F175L
D6	W59A_Y60G_I97V_H136N_I137T_F145G_F156L_F175L
D7	K36E_W59A_Y60G_I97V_H136N_I137T_F145G_F156L_F175L
D8	K36E_C45A_W59A_Y60G_I97V_H136N_I137T_F145G_F156L_F175L
D9	C45A_W59A_Y60G_I97V_H136N_I137T_F145G_F156L_F175L

D10	K36E_C45A_W59A_Y60G_I97V_H136N_I137T_F145G_F156L_K159E_F175L
D11	K36E_C45A_W59A_Y60G_F73W_I97V_H136N_I137T_F145G_F156L_K159E_F175L

3) We have provided a visualization of the substrate tunnel analysis of *Ap*Pgb-wt in the supporting information. Two nonpolar tunnels, one formed by the B/E helices and the second by the B/G helices, provide access to the distal cavity (Ref: *Adv. Microb. Physiol.* **2013**, *63*, 79−96). Previous work by our group on engineering *Ap*Pgb carbene transferases suggested that substrates enter the distal cavity through the B/E helix tunnel. The following **Figure S3** has been added to the supporting information.
4) We have corrected the Figure and Table numbers referred to in the manuscript.

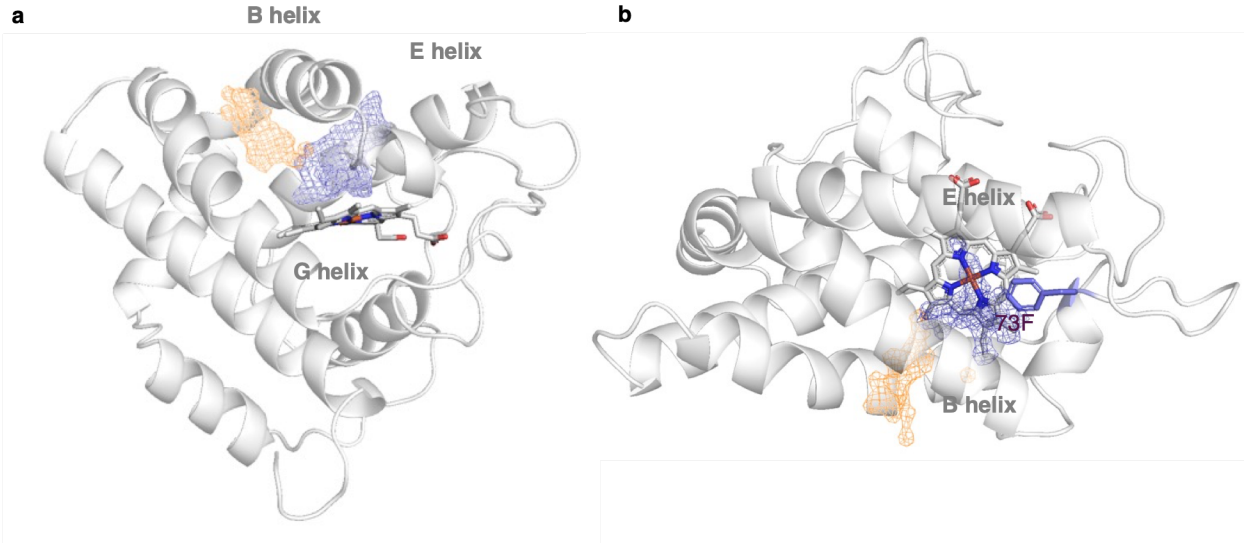

Figure S3. Substrate tunnel analysis of *Ap*Pgb-wt. a, *Ap*Pgb-wt, side view. Analysis made with CAVER. Substrate tunnel between B/E helice (blue), substrate tunnel between B/G helices (organge). **b,** *Ap*Pgb-wt, top view. Highlighted in purple is 73F located at the B/E tunnel.

5. The reviewer writes: "Page 4, lines110-130: The authors describe their combined strategy of site-saturation mutagenesis, random mutagenesis, and a staggered extension process for recombination. … While the overall engineering strategy is clear, it would be helpful to explain which residues were selected for saturation in the SSM approach, as well as how many were selected and why.

Response: We provide a list of residues selected for site-saturation mutagenesis and rationale for the selection. In every round of site-saturation mutagenesis, we chose 8–12 sites-of-interest focusing on active-site residues, substrate tunnel residues, dimer interface residues, residues below the haem cofactor that may have "through-haem impact", and residues where beneficial effects were observed during random mutagenesis. Within each round of SSM, we prioritized residues that are more than 10 sites away from each other, so that they can be potentially recombined later through StEP recombination. However, the exact effect for each residue remains elusive and continues to be an active research interest of the community. Most of the sites screened did not provide any significant improvement. As a result, we would like to leave this information out of the supporting information to avoid misleading interpretation.
Active-site and substrate tunnel residues: 59, 60, 63, 70, 73, 86, 89, 90, 93
Dimer interface residues: 54, 58, 62, 147, 151, 155, 159
Residues below haem cofactor that may have "through-haem impact": 116, 119, 141, 145
Residues that appeared during random mutagenesis: 34, 39, 45, 49, 55, 68, 72, 92, 112, 123, 126, 149, 188, 193, etc.

Note that referee #3 raised a related question regarding our rationale for mutations introduced to the final variant relative to *Ap*Pgb-wt. This information is included in the response below.

6. The reviewer writes: "it would be helpful to add a table to the Supplementary Information with an overview of the wild-type mutations (specific residues), as well as the mutations introduced in variant G8."

Response: We have added **Table S11** and **Table S12** on mutations introduced in each round of evolution. All mutations are compared to ***Ap*Pgb-wt**, with mutations highlighted in red.

Table S11: Summary of mutations introduced in each round of evolution toward ***Ap*Pgb-OxazS-G8-5409**.

Entry	Variant	Mutations from ***Ap*Pgb-wt**
1	***Ap*Pgb-OxazS-G0-5401**	K36E, C45A, W59A, Y60G, F73W, I97V, H136N, I137T, F145G, F156L, K159E, F175L Silent mutations at sites 8, 58, 83, 93, 157, 180
2	***Ap*Pgb-OxazS-G1-5402**	K36E, C45A, W59A, Y60G, F73W, V89T, I97V, H136N, I137T, F145G, F156L, K159E, F175L, P188T Silent mutations at sites 8, 58, 83, 93, 157, 173, 180
3	***Ap*Pgb-OxazS-G2-5403**	K36E, C45A, W59A, Y60G, V63L, F73W, V89T, I97V, V116I, R122S, H136N, I137T, F145G, F156L, K159E, K160R, F175L, P188T Silent mutations at sites 8, 58, 83, 93, 157, 173, 180
4	***Ap*Pgb-OxazS-G3-5404**	K36E, C45A, W59V, Y60G, V63L, F73W, V89T, I97V, V116I, R122S, H136N, I137T, F145G, F156L, K159E, K160R, F175L, P188T Silent mutations at sites 8, 58, 83, 93, 157, 173, 180
5	***Ap*Pgb-OxazS-G4-5405**	K36E, C45A, E54K, W59V, Y60G, V63L, F73W, V89T, I97V, V116I, R122S, H136N, I137T, F145G, F156L, K159E, K160R, F175L, V179A, P188T Silent mutations at sites 8, 58, 83, 93, 157, 173, 180
6	***Ap*Pgb-OxazS-G5-5406**	C45A, E54K, W59V, Y60G, V63L, F73W, V89T, I97V, V116I, R122S, H136N, I137T, F145G, F156L, K159E, K160R, F175L, V179A, P188T Silent mutations at sites 58, 83, 93, 157, 173, 180
7	***Ap*Pgb-OxazS-G6-5407**	C45A, K49S, E54K, W59V, Y60G, V63L, F73W, V89T, I97V, V116I, R122S, H136N, I137T, F145G, F156L, K159E, K160R, F175L, V179A, P188T Silent mutations at sites 58, 83, 93, 149, 157, 173, 180
8	***Ap*Pgb-OxazS-G7-5408**	C45A, K49S, E54K, W59V, Y60G, V63L, F73W, V89T, I97V, D104N, N106D, V116I, R122S, H136N, I137T, R140G, F145G, F156L, K159E, K160R, F175L, V179A, P188T, N193S Silent mutations at sites 58, 70, 83, 93, 115, 149, 157, 173, 180
9	***Ap*Pgb-OxazS-G8-5409**	C45A, K49S, E54K, I55V, W59V, Y60G, V63L, F73W, V89T, I97V, D104N, N106D, V116I, R122S, H136N, I137T, R140G, F145G, F156L, K159E, K160R, F175L, V179A, P188S, N193F Silent mutations at sites 58, 70, 83, 93, 115, 149, 150, 157, 173, 180.

Table S12: Summary of mutations introduced in each round of evolution toward ***Ap*Pgb-StzS-G4-5413**.

Entry	Variant	Mutations from ***Ap*Pgb-wt**
1	***Ap*Pgb-StzS-G1-5410**	C45A, K49S, E54K, W59V, Y60G, V63L, F73W, V89T, R90G, I97V, N106D, V116I, I122S, H136N, I137T, F145G, F156L, K159E, K160R, F175L, V179A, P188T Silent mutations at sites 58, 83, 93, 149, 157, 173, 180
2	***Ap*Pgb-StzS-G2-5411**	C45A, V47I, K49S, E54K, W59V, Y60G, V63L, F73W, S74F, V89T, R90G, I97V, N106D, V116I, I122S, H136N, I137T, F145G, F156L, K159E, K160R, F175L, V179A, P188T Silent mutations at sites 13, 58, 70, 83, 93, 149, 157, 173, 180
3	***Ap*Pgb-StzS-G3-5412**	C45A, V47I, K49S, E54K, L56M, W59V, Y60G, V63L, F73W, S74F, V89T, R90G, I97V, N106D, V116I, I122S, H136N, I137T, F145G, F156L, K159E, K160R, F175L, V179A, P188T Silent mutations at sites 13, 58, 70, 83, 93, 115, 149, 157, 173, 180
4	***Ap*Pgb-StzS-G4-5413**	K16R, L22H, C45A, V47I, K49S, E54R, L56M, W59V, Y60G, V63L, F73W, S74F, V89T, R90G, I97V, N106D, V116I, I122S, H136N, I137T, F145G, F156L, K159E, K160R, F175L, V179A, P188T Silent mutations at sites 13, 58, 70, 83, 93, 115, 149, 157, 173, 180

Additional modifications were made.

1. Page 6, line194: Numbering error.
   Response: We have changed the reference figure of this product inhibition study to (Figure S5) and carefully checked the numbering of reference figures throughout the manuscript.
2. Figure S2: Included information on the ee with which the target oxazolidinone was obtained
   Response: We have added absolute configuration of the desired (*S*)-oxazolidinone products.
3. Page 18 and following: The authors should also include the calculated concentration [mM] of the respective products (can be added to the tables underneath the calibration curves).
   Response: We have added product concentration to all analytical reactions.
4. Page 54: 5-(aminomethyl)-3-(p-tolyl)oxazolidin-2-one (3b): Please indicate if this compound was obtained from a commercial source or synthesized.
   Response: Compound **3b** was synthesized following General Procedure B. We made changes accordingly.
5. Page 61: *tert*-butyl (3-amino-2-hydroxypropyl)(p-tolyl)carbamate (5): The authors describe that this compound was synthesized according to the General Procedure C. However, I couldn't find a description of Procedure C in the SI. Please check and add a detailed description.
   Response: We added General Procedure C.

Referee #2 (Remarks to the Author):

We thank this reviewer for their supportive comments and valuable suggestions.

1. The reviewer writes: "Although they point out also that there exist established routes to this present class

– most notably from the chiral pool building block epichlorohydrin, which is available extremely cheaply as single enantiomers."

Response: Although enantiopure epichlorohydrin can be obtained at about $3/gram, the production of this compound involves epoxidation and subsequent hydrolytic kinetic resolution. The former increases safety concerns in industrial production, and the latter usually results in >50% material loss. Moreover, as listed in Figure S2, all existing methods rely heavily on protecting group manipulation, which results in diminished atom economy. The current industrial synthesis procedure by Pfitzer, shown in Figure S2 equation 5, adopts an imine protecting group strategy. The corresponding reagent derived from chlorohydrin is used in excessive amount and without recycling system. For these reasons, the Gates Foundation actively encouraged our efforts to develop this biocatalytic method, which now provides direct access to the unprotected amine product which could be converted to other pharmacophores divergently. Our work provides a complement to existing synthetic strategies and highlights the benefits of biocatalysis for production of highly polar unprotected products.

2. The reviewer writes: "For the optimization substrate 1a, exhaustive rounds of directed evolution are able to get the yield and ee to excellent levels (Fig 2). They then explore variation of the phenyl ring of the optimization substrate to different substituted phenyls. The outcomes are quite a mix. Although good outcomes can be retained for some simple substitutions (eg p-CO2Me, m-OMe) for many the yields and the ee values decrease quite substantially and overall the scope, even of arene substitution, seems limited. Even though there are a good proportion from Fig 3 which give high ee, often the yields are low to moderate. The addition of a methyl group on the alkene gives only 2% yield and 40% ee, indicating that it has to be a terminal, monosubstituted alkene. The authors comment that this makes it a good starting point for a future campaign but it seems clear that the present system cannot deal with this effectively. In Fig 4 further rounds of evolution are carried out to permit a sulfur atom to be present."

Response: Directed evolution reliably improves activity and selectivity through iterative mutation and screening, accumulating small changes in the macromolecular catalyst that influence the measured properties. This ability to tune the catalysis makes enzymes inherently different from small-molecule catalysts. Thus finding the evolutionary starting point becomes the most important step in the entire evolution campaign for such new-to-nature chemistry: optimization is relatively straightforward once reactivity is found. We would like to emphasize that for medicinally relevant entries (**3u**–**3z**), all the reactions proceeded with excellent enantioselectivity and modest-to-good yields, which sets a solid ground for substrate-specific directed evolution to further improve reaction outcomes. This was demonstrated using **3x** as an example, where we improved the yield from 1% to 24% through four rounds of evolution.

We also respectfully disagree with the reviewer regarding a limitation in substrate scope. A substrate scope is not only a demonstration of excellent examples. We chose to show both good and modest examples because both provide valuable information. Deleting 6 examples of low enantioselectivity entries will certainly make the substrate scope looks better, but it will diminish the depth of the discussion.

3. The reviewer writes: "The title sounds quite broad but the space within which the reaction operates is narrow."

Response: We believe this title covers three aspects of the manuscript: the synthetic goal (chiral oxazolidinone), the chemistry (aziridination of unactivated alkenes), and the strategy (biocatalytic nitrene transfer).

4. The reviewer writes: "Furthermore in the past couple of years there have been several asymmetric aziridination processes which operate very effectively on unactivated terminal alkenes with broad scope. For example, ref 36 in the submission, but also a paper which is not cited here (unless I missed it) from

Baik and Blakey (JACS, 2024, 146, 1447) using Rh catalysis. Therefore, it is difficult to say this is unaddressed problem in the literature."

Response: One of the key challenges of our work is asymmetric NH aziridination. First, the coordinative nature of the free amino group may lead to poisoning of transition-metal catalysts. Moreover, without the sulfonyl substituent, asymmetric free NH aziridination requires more precise control of the chiral environment. Both challenges can be hard to address *via* chemical methods. The hydrogen bonding network as well as the programmable active-site geometry of enzymes are well-suited to address both challenges. This reference has been added to the citation list.

5. The reviewer writes: "The rather restricted substrates that this delivers good results on (i.e. an N-Boc, N-aryl allyl amine, with relatively limited possibility to move away from phenyl as the aryl group) means that it is not of the broad interest and impact level needed to justify publication in Nature, in this reviewers opinion. It is a nice study that is well executed. It is clear that a huge amount of work went into the directed evolution studies. But my opinion is that publication in JACS or ACS Central Science would more appropriate for the reasons stated above."

Response: We appreciate the reviewer's comment from a synthetic point view. But we respectfully disagree regarding the substrate limitation. First, *N*–Boc is *not a protecting group*, but rather a reacting component **required** to contribute to the final product. Second, according to SAR study, *N*–allyl is leading to the medicinally **required** *aminomethyl* group for good antibiotic activity. Third, the *N*-aryl group was chosen because it is **required** for the antibiotic activity. We chose this substrate scope because they are the most medicinally relevant. With the activity established in this work, we can steer the enzyme toward more diverse substrate classes using directed evolution when a new substitution pattern proves critical for the antibiotic activity. Ref 5 (SAR study): *Angew. Chem. Int. Ed.* **42**, 2010–2023 (2003).

From a synthetic point of view, we believe this biosynthetic strategy excels as the first *asymmetric catalysis* strategy for the production of these medicinally relevant molecules while avoiding explosive materials, organic solvents, and functional group interconversion. But the key advance of this work is *not limited to synthetic strategy*. The asymmetric NH aziridination of unactivated alkenes is new to any existing enzymes or small molecule catalysts. The fact that this enzyme can enable both aziridination and ring expansion, two completely different reactions in a cascade, is very unusual for known biocatalysts, which we now explain in more detail computationally (referee #3 comment 8, supporting information Figure S27–28). We believe this work will be inspiring for the biocatalysis community with respect to pursuing challenging transformations.

Referee #3

The manuscript titled "Biocatalytic Nitrene Transfer Enables Aziridination of Unactivated Alkenes for the Synthesis of Chiral Oxazolidinones" by Frances H. Arnold and coworkers reports the development of a novel biocatalyst, OxazS G8, for the enantioselective production of chiral oxazolidinones from inert alkenes via directed evolution of a heme-containing protein. Using both experimental optimization and computational analyses (DFT and MD), the authors demonstrate that this new enzyme efficiently catalyzes nitrene transfer and aziridination, opening promising possibilities for the direct and sustainable synthesis of clinically important antibiotics. The work is of high interest and, in my opinion, suitable for publication in Nature, but the clarity and impact of the manuscript would benefit from addressing the following minor points.

1. The reviewer writes: "The authors observe a dramatic increase in reaction yield upon optimization of the experimental conditions for OxazS-G8. This improvement would be more informative if the same optimization protocol were also applied to the earlier OxazS-G8 variant that already achieved high

enantioselectivity but much lower yield (Figure 2), to clarify whether the yield boost is primarily due to the new mutations or mainly to condition screening."

Response: This condition optimization benefits most variants in the lineage. But the new mutations introduced to OxazS-G8 were also important for the observed improvement.

	R1 P	R1 IS	R2 P	R2 IS	R3 P	R3 IS	R1 yield (%)	R2 yield (%)	R3 yield (%)	Average yield (%)	Previous yield (%)	Increase Y/N
G0	80.3	946.3	85.4	1014.7	74.7	1034.3	10.7	10.6	9.1	10.1	6	yes
G1	136	983.2	142.3	1048.5	131.6	1062.9	17.4	17.1	15.6	16.7	12	yes
G3	171.5	1002	173.2	1025.4	183.8	1021.2	21.5	21.2	22.6	21.8	18	yes
G4	277.2	990.7	289.7	988.1	287.3	1004.4	35.2	36.8	35.9	36.0	28	yes
G5	185.6	1050.3	221.5	1062.3	213.4	1045.6	22.2	26.2	25.6	24.7	22	yes
G6	390.7	1021.8	383.7	1023.5	375.2	995.5	48.0	47.1	47.4	47.5	27	yes
G7	338.5	1059.7	316	969.3	291.7	1000	40.1	41.0	36.7	39.3	32	yes

2. The reviewer writes: "The computational studies focus on OxazS-G2 and OxazS-G3, but the rationale for selecting these specific variants is currently unclear. A brief explanation of why these were chosen for detailed analysis, rather than other members of the directed evolution trajectory, would help the reader follow the computational strategy."

Response: We thank the reviewer for this suggestion. In the evolutionary trajectory, a single mutation, A59V incorporated in the third round of evolution, gave the greatest improvement of enantioselectivity from 53% (OxazS-G2) to 94% *ee* (OxazS-G3) (Figure 2a). Therefore, the computational studies were performed by comparing the OxazS-G2 and OxazS-G3 variants to understand the role of this critical A59V mutation in improving the enzymatic enantiocontrol. We have added a brief explanation of this rationale to the revised manuscript.

3. The reviewer writes: "The A59V mutation is close to the active site and appears important, but the roles of more distal mutations remain less clear. A more detailed discussion of whether these distal changes could exert allosteric effects, and how that might influence reactivity or selectivity, would add value to the mechanistic interpretation."

Response: It is important to note that directed evolution works by accumulating incremental, small improvements *via* iterative mutation and screening; small improvements are expected in each round, and they are often difficult to rationalize. As is also the case in classical enzymology, it is extremely difficult, even having crystal structures of the catalysts, to determine how mutations interact with previous mutations to alter function.

Over the past few years, empirical data accumulation on this relatively new enzyme scaffold has allowed us to formulate a few very general rationales for mutations at selected sites of interest. The following **Figure S7** describes our proposed rationales, but these are rationales rather than recipes.

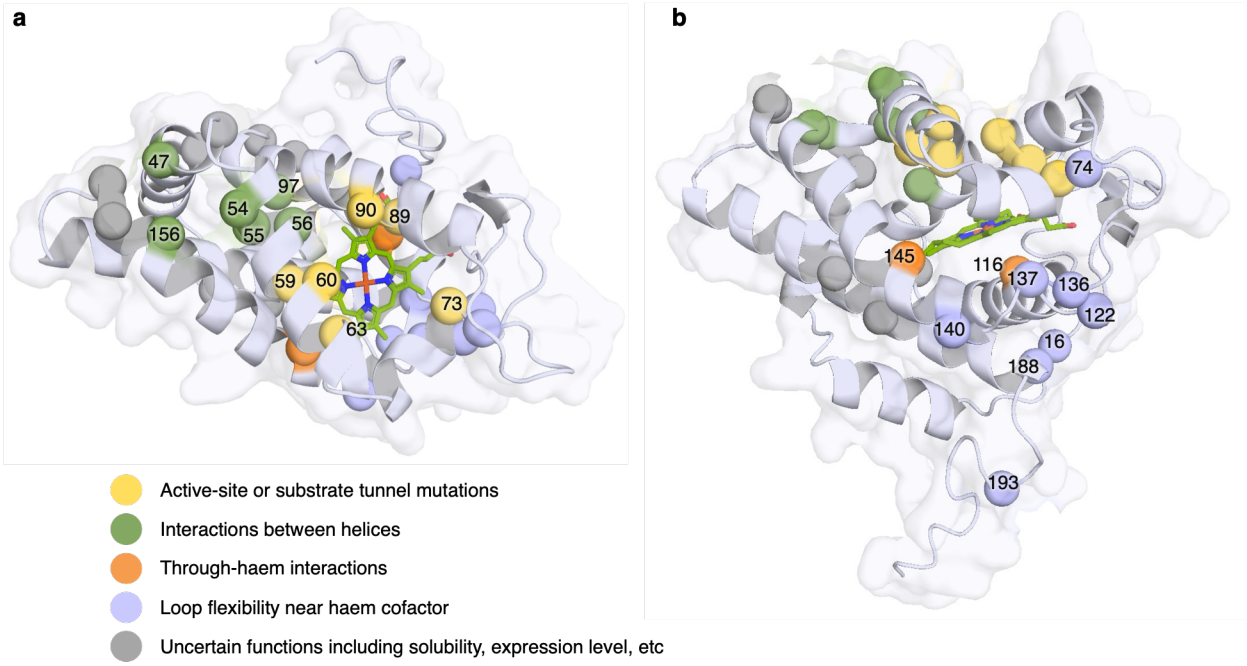

Figure S7. Proposed rationale for the effects of mutations introduced to *Ap*Pgb-OxazS-G8 and *Ap*Pgb-StzS-G4. **a,** Top view. **b,** Side view.

We also attempted to address this reviewer's comment experimentally. We don't think performing "alanine scan" for all of the *individual* mutations introduced through evolution is very informative. Instead, we have performed a StEP recombination (a DNA reshuffling technique for back-crossing) between OxazS-G8 and OxazS-G0. We then performed every-variant sequencing for the 400 variants screened. The following table shows the *plate-screening* results (OD_{600} and catalyst loading not controlled) of variants with fewer than 5 mutations. Mutations such as N193F, P188S_N193F, D104N_N106D, E36K, E36K_K49S have minor impacts on reactivity in the OxazS-G8 background. On the other hand, V89T (located at the substrate tunnel) significantly impacts both yield and activity, while the E36K_K43E pair may rescue the activity loss without V89T. R181Q (located underneath heme cofactor) is critical for the yield. V116I_R122S located close to the axial ligand, may be slightly beneficial to the enantioselectivity.

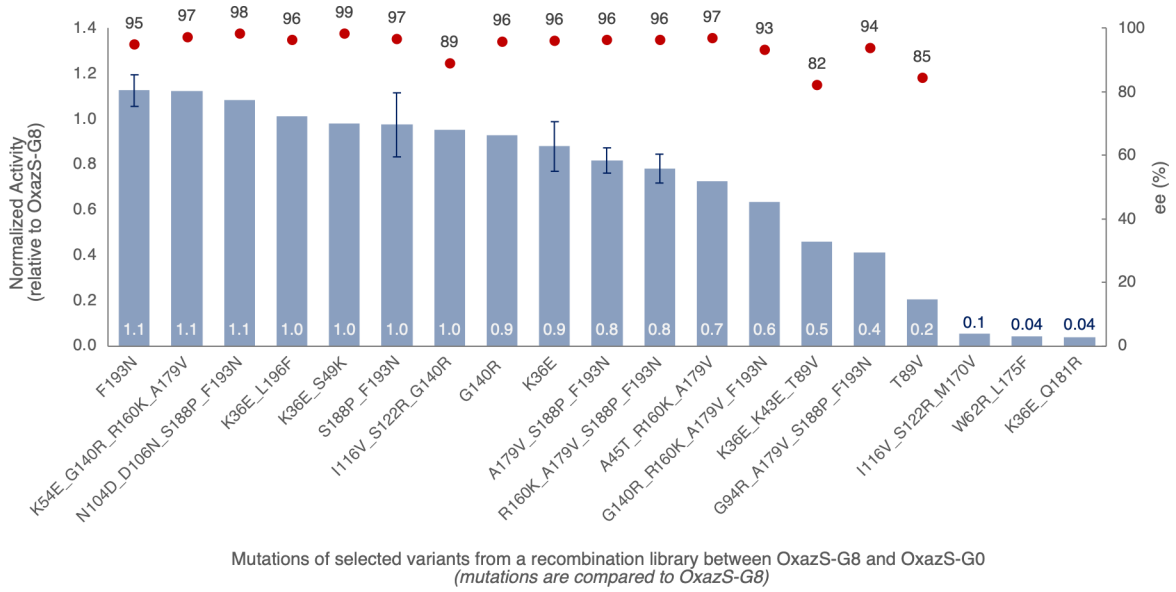

Mutations of selected variants from a recombination library between OxazS-G8 and OxazS-G0
(mutations are compared to OxazS-G8)

4. The reviewer writes: "A table summarizing the atomic spin populations obtained from DFT calculations would be helpful for tracking the distribution of unpaired electrons throughout the reaction pathway and clarifying the electronic structure changes along the nitrene transfer and aziridination steps."

Response: We thank the reviewer for this suggestion. We have added a figure (Figure S10) summarizing the atomic spin densities obtained from the DFT calculations for the key intermediates and transition states along the reaction pathway. These results highlight the radical character on the N atom of the Fe nitrene (^{3}**I**) and on the secondary alkyl radical carbon in the ring-opening intermediate ^{3}**II**.

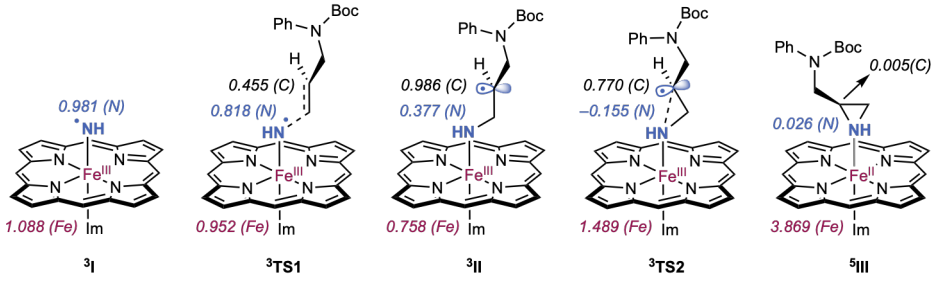

5. The reviewer writes: "It would be informative to know whether kinetic rate constants can be extracted from the experimental data. If so, quantifying the catalytic improvement of the evolved variants relative to earlier ones would greatly strengthen the mechanistic narrative. If computed rates are available, it would also be useful to know which step is predicted to be rate-determining in the current variant."

Response: 1) In general, the reaction proceeds relatively slowly, requiring 20 h of reaction time. We reasoned this is because the reaction requires two cascade steps, the aziridination and ring-expansion step. Initial rate experiments on ***Ap*Pgb-OxazS-G0** and ***Ap*Pgb-OxazS-G8** showed a 4-fold increase in initial rate for the evolved variant (see below). But initial rate is not a comprehensive descriptor. Substrate-specific evolution can improve k_{cat} and K_M. But other factors such as enzyme expression level, as well as protein stability and solubility all contribute to the final reaction yield using cell lysate.

2) In our experience, the rate-limiting step is usually the nitrene formation step. Due to extensive hydrogen-bonding interactions required to achieve this elementary step, it is hard to elucidate this step with a truncated

DFT model. But we agree with the reviewer that it could be very valuable to address this question *via* a more specialized computational study.

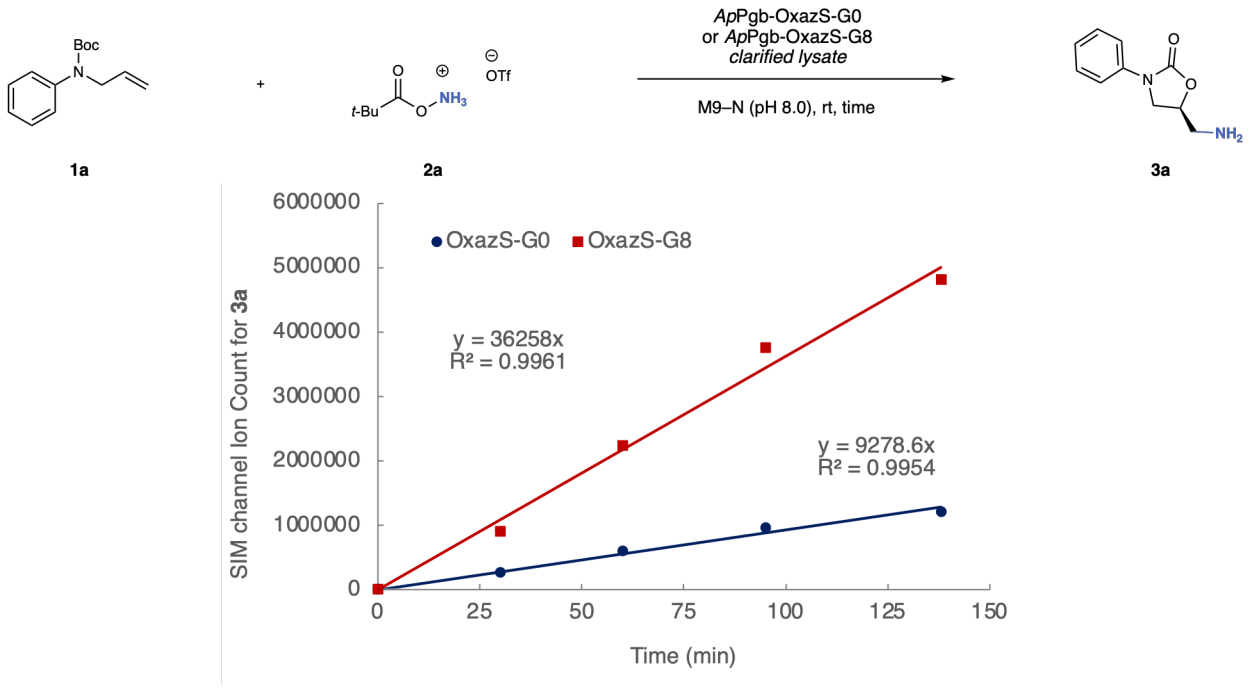

Figure S6. Initial Rate Experiments Comparing ***Ap*Pgb-OxazS-G0** and ***Ap*Pgb-OxazS-G8**. Reaction performed at standard conditions: **1a** (5.0 mM), **2a** (10.0 mM) with 5% v/v EtOH as co-solvent. Analysis based on single ion mass channel ion count integrations of **3a**.

6. The manuscript highlights a CH-π interaction that is said to be important for the reaction. Because such interactions are typically weak and have some electronic character, it would be helpful to clarify how their strength was assessed in the MD simulations and how confident the authors are that the chosen force field captures this effect adequately.

Response: We thank the reviewer for this comment. In this study, the strength of the C–H···π interaction was assessed based on the C–H···π distance to the centroid of the F93 side chain benzene ring. In the (*Re*)-face attack structures, the relatively short most populated C–H···π^{F93} distance (3.36 Å) indicates that this interaction is stronger than those in the (*Si*)-face attack structures, which have a longer most populated C–H···π^{F93} distance of 3.96 Å (see Figure S19E for the detailed distance distributions). This C–H···π interaction is enabled by the observed substrate binding poses (Figure 2e) that place the conformationally flexible *N*-allyl group in proximity to the F93 side chain. In our MD simulations, we used the second-generation general Amber force field (gaff2) and DFT-derived RESP charges for the substrate and the ff19SB force field for the protein, which includes the F93 residue. These force field parameters describe the C–H···π interaction in a combination of Lennard–Jones (LJ) potential and a fixed charge electrostatic model. Based on previous benchmark studies (e.g., *J. Comput. Chem.* **2009**, *30*, 2187), AMBER ff99 force field, similar to the ff19SB force field used in the present study, correctly predicts a shallow well for weak C–H···π interactions.

7. The MD protocol used to compare OxazS-G8 and StzS-G4 is notably different from the one applied elsewhere. A more consistent treatment across variants would aid direct comparison. In addition, showing computed tunnels on protein structures would help illustrate how the active site environment differs between these systems.

Response: We thank the reviewer for these suggestions. To ensure consistency, we have re-performed the MD simulations of **OxazS-G8** and **StzS-G4** using the same protocol applied to the other variants (three independent 500-ns replicas per system in AMBER using the same force field parameters and minimization/heating/equilibration/production run workflow). We have updated all relevant figures and discussions in the SI (Figures S22–S25) using the latest results from the MD protocol consistent with other simulations in this study. The overall conclusions regarding **OxazS-G8** and **StzS-G4** variants are not affected when using this new protocol. A wider tunnel opening in **StzS-G4** was still observed.

We have added an ensemble tunnel analysis using CAVER Analyst 2.0. Visualization of substrate entrance tunnels (Figure S26A and S26B) and the computed bottleneck radii of the two variants (Figure S26C) demonstrates that the **StzS-G4** variant has a wider tunnel with a greater bottleneck radius than the **OxazS-G8** variant.

8. The role of the enzyme in the ring-expansion step is not fully explained. A more detailed description of how the protein environment facilitates (or avoids inhibiting) this step would improve understanding of the downstream transformation.

Response: We thank the reviewer for this suggestion. We have added additional DFT and MD results to reveal how the enzyme environment promotes the aziridinium ring opening (see Figures S27 and S28 and the corresponding discussion). In short, the DFT calculations revealed that, in the absence of enzyme, an energy penalty of 4.8 kcal/mol is needed to isomerize the non-productive *gauche* conformer of the aziridinium (**IV**) to the productive *anti* conformer needed for the S_N2 ring-opening transition state. By contrast, the MD simulations revealed that in the enzyme active site, the productive *anti* conformation of the aziridinium is frequently accessed in 5.3% of the MD structures, despite their relatively high energy based on DFT calculations. These results indicate that the enzyme environment promotes the S_N2 ring-opening by stabilizing the productive *anti* conformer prior to the ring opening. More details on the active site residue–substrate interactions that stabilize the *anti* conformer of the aziridinium are provided in Figure S28.
This interpretation highlights that the enzyme can promote both the aziridination and the ring-expansion steps within the evolved active site. This information is valuable in that it provides a mechanistic rationale for this complex cascade reaction, paving the way for future application of biocatalytic nitrene transfer in complex bond formation reactions.

9. The blue surfaces shown in Figure S10 are not clearly described in the caption or main text. A brief explanation of what these surfaces represent (e.g., cavities or some other property) would be useful.

Response: The blue surfaces represent the active site cavities generated using PyMOL. We have added this information to the caption of this figure, which is now Figure S15.

10. The confidence scores of the AF3-predicted structures should be provided.

Response: The global pLDDT score for the AF3-predicted structure for ***Ap*Pgb-OxazS-G8** is 91.38. The global pLDDT score for the AF3-predicted structure for ***Ap*Pgb-StzS-G4** is 91.29. We added these two numbers to the footnote of Figure 2 and Figure 4, respectively. The loop regions at the N-terminus and the C-terminus $His_{\times 6}$ tag has low confidence score. To better visualize the data, we added Figure S8 showing the color-coded structure of both enzymes based on b-factors. Summary tables of pLDDT scores of both enzymes are included in Table S13, and Table S14. We can also provide a per-residue pLDDT score upon request.

11. The time evolution plots in Figures S11 and S13 show 0-1500 ns on the x-axis, but the trajectories appear to cover only 500 ns per replica. For clarity, I suggest rescaling the x-axis to 0-500 ns for each

replica. In addition, the red line in these panels appears to represent a running average across replicas, which is misleading. It would be preferable either to show individual replicas distinctly or to clarify that the red line is an across-replica average.

Response: We thank the reviewer for pointing this out. These figures (now Figures S16 and S18) have been updated according to the reviewer's suggestion to show each replica in a separate panel.

12. The phrase "classical MD" is somewhat redundant, as MD simulations in this context are inherently classical, force field-based methods. Unless the study involved hybrid or quantum mechanical MD approaches, it would be more appropriate to simply refer to "MD" or reserve "classical MD" only when explicitly contrasting with quantum or ab initio MD.

Response: We thank the reviewer for this comment. We have replaced "classical MD" with "MD" throughout the manuscript and Supplementary Information. In each document, the word "classical" was only used once when we first introduced the method.

13. The AMBER topologies, coordinates, and simulation input files should be deposited in an open access repository or provided as part of the supplementary data to ensure full reproducibility of the computational results.

Response: We thank the reviewer for this suggestion. All AMBER topology files, coordinate files, MD input files, and representative snapshots have been deposited in the Zenodo open-access repository under DOI: 10.5281/zenodo.21496297. A corresponding data availability statement has been added to the revised manuscript.